

Stability Analysis and Effect of CES on ANN Based AGC for Frequency Excursion

J.Raja[†] and C.Christober Asir Rajan*

Abstract – This paper presents an application of layered Artificial Neural Network controller to study load frequency control problem in power system. The objective of control scheme guarantees that steady state error of frequencies and inadvertent interchange of tie-lines are maintained in a given tolerance limitation. The proposed controller has been designed for a two-area interconnected power system. Only one artificial neural network controller (ANN), which controls the inputs of each area in the power system together, is considered. In this study, back propagation-through time algorithm is used as neural network learning rule. The performance of the power system is simulated by using conventional integral controller and ANN controller, separately. For the first time comparative study has been carried out between SMES and CES unit, all of the areas are included with SMES and CES unit separately. By comparing the results for both cases, the performance of ANN controller with CES unit is found to be better than conventional controllers with SMES, CES and ANN with SMES.

Keywords: Artificial Neural Network, Automatic Generation Control, Capacitive Energy Storage, Stability Analysis, Superconducting Magnetic Energy Storage

1. Introduction

Automatic Generation Control (AGC) is one of the most important issues in electric power system design, operation and control. The objective of the AGC in an interconnected power system is to maintain the frequency of each area and to keep tie-line power close to the scheduled values by adjusting the MW outputs the AGC generators so as to accommodate fluctuating load demands. The AGC design with better performance has received considerable attention during the past years and many control strategies have been developed for AGC problem. The controller based on classical control theories employed as in [1]-[4] are insufficient because of changes in operating points while the loads change continuously during daily cycle, which is an inherent characteristics of power system. The variable structure controllers proposed as in [5], [6] are used to overcome this problem. On the other hand many adaptive is control techniques have been proposed for AGC [7]-[10]. Due to the requirement of the perfect model, which has to track the state variable and satisfy system constraints, it is rather difficult to apply these adaptive control techniques to AGC in practical implementations. These controllers are considerably slow because the estimation of parameter is needed and more computation is required.

In this paper, ANN controller is used because this controller provides faster control than the others using conven-

tional, adaptive control techniques. ANN controller gives a short settling time and eliminates the necessity of parameter estimation time required in conventional adaptive control technique. The model of nonlinear controller which is the most suitable model to represent the real system is given by a set of differential equations, which is the most suitable model to represent the real system. As ANN configuration will be used to control the non linear system. So back propagation through time algorithm is preferred in the ANN controller to cope with the continuous time dynamics [11]-[13]. This algorithm in a way gives control rule. Even though multi layer perception is non recurrent, when more than one of this structure is used with back propagation through time algorithm, it can be perceived as a recurrent ANN. Thus this study, as the system equations are used to model the system, there is no need to train ANN to obtain system model.

It is well known that AGC system conventionally includes an integral controller as secondary controller. The integral gain set to level the compromise between fast transient recovery and low overshoot in dynamic response of the system [14]. Unfortunately, this type of controller even if its gain is optimized is considerably slow and therefore the recovery of transient in the power system with respect to load perturbation takes very long time. The considered power system includes two areas of the that consist of two steam turbine.

The interconnected power system with two areas contains SMES units in each area. Addition of a small capacity SMES unit to the system sufficiently improves transients of frequency and tie line power deviation against to small load disturbances. In the SMES unit a small magnetic coil is connected to the ac grid through a power conversion unit, which includes converter and inverter. The super conduct-

[†] Corresponding Author: Dept. of Electrical and Electronic Engineering, Sri Manakula Vinayagar Engineering College, Affiliated to Pondicherry University, Madagadipet – 605 107, India. (rajaj1980@rediff.com)

* Dept. of Electrical and Electronic Engineering, Pondicherry Engineering College, Pondicherry, India.(asir_70@hotmail.com)

Received: April 23, 2010; Accepted: July 23, 2010

ing coil can be charged to set a value from the grid during normal operation of the power system. Once coil is charged, it conducts current with virtually no losses. When there is any sudden rise in demand, the stored energy is almost released through energy conversion device to the power system as an alternating current. The stored energy is taken about 20 MJ and 30 MJ because of factor of super conductor stability. To damp out the oscillations as fast as possible, both the effect of SMES and CES based ANN using back propagation through time algorithm are investigated together. For the simulation, step disturbance is included in both areas, the considered power system is controlled by using (i) Conventional integral controller. (ii) ANN using back propagation through time algorithm.

The application of SMES to electric power system can be grouped into two categories. (i) Large scale energy storage like conventional pumped hydro plant storage to meet for sudden load leveling applications. (ii) Low capacity storage to improve the dynamic performance of power system. In first case large sized (hundreds of meters in diameter) high capacity super conducting magnetic energy storage capable of storing 10^8 MJ is necessary [15]-[18], for the second application, very small sized SMES units with storage capacity of the order of 10^2 MJ or even less would be sufficient for a small load disturbances and with the optimized gain for the integral controller, the power frequency oscillation and the tie line deviation persist for a long duration, the addition of a small capacity SMES unit to the system sufficiently improves this situation and the oscillations are practically damped out.

The use of SMES and CES for load leveling application and for improvement of the dynamic performance of power system has been described in [18]-[21] The importance of control system using SMES has been presented as one of the powerful stabilizers for undamped oscillations which tends to occur in a long distance bulk power transmission system which has been viewed and analyzed in the literature [22]. In [23] the improvement in AGC with the addition of a small capacity SMES unit is studied, and time domain simulations used to study the performance of the power system dynamics are analyzed. Their applications in real power have invited problems from the view points of operation, maintenance, cost but the only advantages of SMES is, that is very much useful for high power applications.

The battery energy storage for power system dynamic performance improvement has been widely and vividly reported as in [24], [25]. Their applications in real power system have invited problems from the view points of operation, maintenance and cost involvement. However, capacitive energy storage (CES) [26] may be a better alternative choice to damp out the power frequency oscillation, following any perturbation in the power system. CES is, practically, maintenance free. Unlike magnetic energy storage units, CES does not impose any environmental problem. The operation is quite simple and less expensive, compared to SMES. SMES requires a continuously operating liquid helium system. In magnetic storage systems, continuous flow of current is required but CES does not

demand so. Thus, as a corrective measure against power system perturbation, CES plays an important role to damp out local mode power system oscillations.

The objectives of the proposed works are: (i) to obtain the transient performance of the coordinated action of two areas AGC loop with various load conditions. (ii) To investigate the further impact of SMES on the same transient performance, control system using SMES has been presented as one of the powerful stabilizers for damping out the power system oscillations. (iii) To investigate the impact of CES on the same transient performance, Control system using CES has been presented as one of the powerful stabilizers for damping out the power system oscillations. (iv) To compare the coordinated action of the transient performance of AGC and ANN with SMES and without SMES. (v) To compare the coordinated action of the transient performance of AGC and ANN with CES and without CES. (vi) Finally comparative analysis has been carried between AGC and ANN with coordinated action of SMES and CES.

The organization of the paper documented in the following headings. Section 2 provides two area power system investigations. While section 3&4 dealing with mathematical modeling of SMES and CES. Section 5 incorporates ANN in AGC. Section 6 including Stability analysis comparison with PI, SMES, CES. Section 7 Deals with result analysis being followed by concluding remarks.

2. AGC In Two-Area Power System

The two area power system, including two single areas connected through a tie-line is considered. Each area supplies its user pool, and tie-line allows electric power to flow between areas. So, both areas affect each other (i.e., a load perturbation in one area affects the output frequencies of both areas as well as power flow on the tie-line). Because of this, the control system of each area needs information about the transient situation in both areas to bring the local frequency to its steady state value. As the information about each area is found in its output frequency, the information about the other area is in the perturbation of the tie-line power. So, tie-line power flow is needed in order to feed back the information in both areas. While the electric load increases in one area, the frequency of the same area decreases, and power transmitted from the other area to this area increases. In conventional systems, the turbine reference power of each area is tried to be set to its nominal value by an integral controller. The input of the integral controller of each area is $B_i \Delta f_i + \Delta P_{tie}$ ($i = 1, 2$), and it is called area control error (ACE). The parameters of B_i may be optimized, but here, they are chosen as $1/K_{pi} + 1/R_i$ as generally taken. The equations are:

$$\Delta F_1(k+1) = \Delta f_1(k) + (T_s / T_{p1}) * (K_{p1} * \Delta P_{t1}(k) - K_{p1} * \Delta P_{e1} - \Delta f_1(k) - K_{p1} * \Delta P_{12}(k)) \quad (1)$$

$$\Delta P_{t1}(k) + (T_s / T_{t1}) * (K_{t1} * \Delta P_{h1}(k) - \Delta P_{t1}(k)) \quad (2)$$

$$\Delta P_{12}(k+1) = \Delta P_{h1}(k) + (T_s/T_{h1}) * (K_{h1} * \Delta P_{ref1}(k) - (K_{h1}/R_1) * \Delta f_1(k) - \Delta P_{h1}(k)) \quad (3)$$

$$\Delta f_{12}(k+1) = \Delta P_2(k) + (T_s/T_{p1}) * (K_{p1} * \Delta P_{12}(k) - (K_{p1} * \Delta P_{e2}) - \Delta f_2(k) - K_{p1} * \Delta P_{21}(k)) \quad (4)$$

$$\Delta P_{12}(k+1) = \Delta P_{12}(k) + (T_s/T_{l2}) * (K_{l2} * \Delta P_{h2}(k) - \Delta P_{12}(k)) \quad (5)$$

$$\Delta P_{h2}(k+1) = \Delta P_{h2}(k) + (T_s/T_{h2}) * (K_{h2} * \Delta P_{ref2}(k) - (K_{h2}/R_2) * \Delta f_2(k) - \Delta P_{h2}(k)) \quad (6)$$

$$\Delta P_{12}(k+1) = 2 * \pi i * T_{12} * T_s * (\Delta f_1(k) * \Delta f_2(k)) + \Delta P_{12}(k) \quad (7)$$

$$\Delta P_{12}(k+1) = 2 * \pi i * T_{12} * T_s * (\Delta f_2(k) - \Delta f_1(k)) + \Delta P_{21}(k) \quad (8)$$

$$\Delta P_{ref1}(k+1) = \Delta P_{ref1}(k) - (K_{i1} * T_s) * (\Delta P_{12}(k) + B_1 * \Delta f_1(k)) \quad (9)$$

$$\Delta P_{ref2}(k+1) = \Delta P_{ref2}(k) - (K_{i2} * T_s) * (\Delta P_{21}(k) + B_2 * \Delta f_2(k)) \quad (10)$$

3. SMES System

Fig. 1 shows the transfer function model SMES unit contained DC Superconducting coil and converter which are connected by Star-Delta/Delta-Star transformer. The control of the converter firing angle provides the DC voltage E_d appearing across the inductor to be continuously varying within a certain range of positive and negative values. The inductor is initially charged to its rated value I_{do} by applying a small positive voltage. Once the current reaches the rated value, it is maintained constant by reducing the voltage across the inductor to zero since the coil is [24-25] superconducting. Neglecting the transformer and the converter losses, the DC voltage is given by equation (11) where E_d is DC voltage applied to the inductor (KV), α is firing angle ($^\circ$),

$$E_d = 2V_{do} \cos \alpha - 2I_d R_c \quad (11)$$

I_d is the current flowing through the inductor (KA), R is the equivalent commutating resistance (ohm) and V_{do} is maximum circuit bridge voltage (KV). Charge and discharge of SMES unit are controlled through change of commutation angle. If α is less than 90° , converter acts in rectifier mode and if α is greater than 90° , the converter acts in inverter mode. In this study, as in recent literature, inductor voltage deviation of SMES unit of each area is based on error of the same area in power system. Moreover the inductor current deviation is used as a negative feedback signal in SMES control Loop. So the current variable

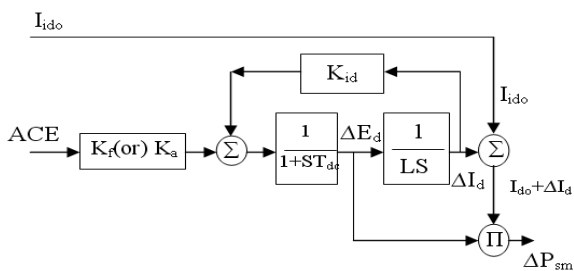


Fig. 1. Transfer Function Model of SMES.

of SMES unit is intended to be settling its steady state value. If the load demand changes suddenly, the feed back provide the prompt restoration of current. The inductor current must be restored to its nominal value quickly after system disturbances, so that it can respond to the next load disturbance immediately. As a result, the equations of inductor voltage deviation and current deviation for each area in Laplace domain are as follows:

$$\Delta E_{di}(s) = K_{oi} \frac{1}{1+ST_{dci}} \Delta f_i(s) - K_{idi} \frac{1}{1+ST_{dci}} * \Delta I_{di}(s) \quad (12)$$

$$\Delta I_{di}(s) = \frac{1}{SL_i} \Delta E_{di}(s) \quad (13)$$

Where, K_{idi} is the gain for feedback. $\Delta I_{di}, T_{dci}$ is the change in increasing current, converter time delay, K_{oi} (KV/Unit) is gain constant and L_i (H) is the inductance of the coil. The deviation in the inductor real power of SMES unit is expressed in time domain as follows.

$$\Delta P_{smi}(t) = \Delta E_{di} I_{dio} + \Delta I_{di} \Delta E_{di} \quad (14)$$

This value is assumed positive for transfer from AC grid to DC. The energy stored in SMES at any instant in time domain is given as follows.

$$W_{smi}(t) = \frac{L_i I_{di}^2}{2} \text{ (MJ)} \quad (15)$$

3.1 Frequency Deviation as a Control Signal

The frequency deviation Δf of the power system is sensed and used to control the SMES voltage, E_d . When power is to be pumped back in to the grid in the case of fall in the frequency due to sudden loading in the armature, the control voltage E_d is to be negative since the current through the inductor and thyristor cannot change its direction. The incremental change in the voltage applied to the inductor is expressed as:

$$\Delta E_d = \left[\frac{K_f}{(1+ST_{dc})} \right] * \Delta f \quad (16)$$

Where: $i,j=1,2$, ΔE_d is the incremental change in converter voltage, T_{dc} is the converter time delay, K_f is the gain of the control loop and S is the Laplace operator d/dt . If ACE is used as control signal then.

$$\Delta E_d = \left[\frac{K_f}{(1+ST_{dc})} \right] * \{ K_{Ai} (\Delta f_i + \frac{1}{B_i} \Delta P_{ij}) - K_{Iai} \Delta I_{di} \} \quad (17)$$

3.2 Area Control Error (ACE) As Control Signal

In case where tie line power deviation signals are available, it may be desirable to use area control error as input

to SMES control logic. This has certain disadvantages, which are desirable later, compared to frequency deviation derived controls. The area control error of two areas is defined as:

$$ACE_i = \Delta P_{ij} + B_i * \Delta f_i \quad (18)$$

Where, $i,j=1,2$, Δf_i = Change in frequency of area, i . ΔP_{ij} = Change in tie line power flow out of area i to j . If ACE is directly used for the control of SMES, The gains constant K_A (KV/unit Area) would be totally different from K_F , the gain constant for frequency deviation as control signal. So a signal proportional to area control error ($\Delta f_i + (1/B_i) * \Delta P_{ij}$) is used in such a scheme. Then,

$$\Delta E_{di} = \frac{K_{Ai}}{(1 + S T_{dci})} (\Delta f_i + \frac{1}{B_i} * \Delta P_{ij}) \quad (19)$$

The discrete time equations for the two area AGC including SMES is solved in MATLAB using m-file and the results are presented here. The sampling time T_s is 0.0001. The equations of SMES for two area in discrete form are:

$$\Delta E_{di}(k+1) = \Delta E_{di}(k) + (T/T_{dc}) * (B_i * \Delta f_i + \Delta P_{tie}) * K_{oi} - \Delta I_{di} * K_{id} - \Delta E_{di}(k) \quad (20)$$

$$\Delta I_{di}(k+1) = \Delta I_{di}(k) + \Delta I_{dio} \quad (21)$$

$$\Delta P_{smi}(k+1) = \Delta E_{di}(k+1) * (\Delta I_{di}(k+1) + \Delta I_{dio}) \quad (22)$$

4. Capacitive Energy Storage

Capacitor is an electro chemical device consisting of two porous electrodes, an ion exchange membrane separating the two electrodes and a potassium hydroxide electrolyte. In many ways, an ultra capacitor is subject of same physics as a standard capacitor. That is the capacitor is determined by [24]-[26] the effective area of the plates, the separation distances of the electrode and the dielectric constant of the separating medium.

Fig. 2 shows transfer function model of CES. The operation of CES units, that is, charging, discharging, the steady

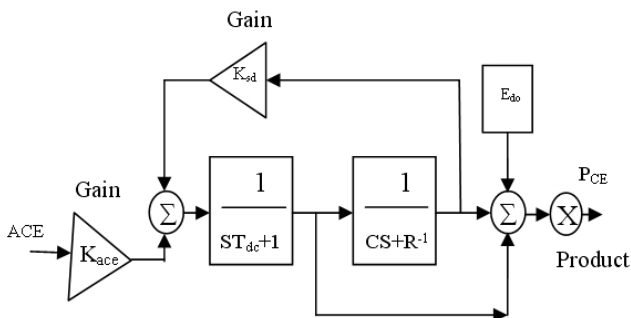


Fig. 2. Transfer function model of CES.

state model and the power modulation during dynamic oscillatory period, is controlled by the application of the proper voltage to the capacitor so that the dsired current flows in to or out of the CES. This can be achieved by controlling the firing angle of the converter bridges. Neglecting the transformer and the converter losses, the DC voltage is given by [22]

$$E_d = 2V_{do} \text{Cos}\alpha - 2I_d R_c \quad (23)$$

Where: E_d =DC voltage applied to the capacitor (Kv), α =firing angle(degree), I_d =current through the capacitor(KA), R_c =equivalent commutating resistance(ohm), V_{do} =maximum open circuit bridge voltage of each 6-pulse converter at $\alpha=0$ (Kv).

The capacitor is initially charged to its normal voltage, E_{do} by the PCS. Once the voltage of the capacitor has reduced E_{do} , it is kept floating at this voltage by continuing supply from the PCS to compensate for the dielectric and other leakage losses of the capacitor. The energy stored at any instant,

$$W_r = \frac{CE_d^2}{2} \text{ (MJ)} \quad (24)$$

Where C =Capacitance of CES (Farad).

4.1 Frequency Deviation as Control Signal

The frequency deviation Δf of the power system is sensed and used to control the CES current I_d . The incremental change in CES current is expressed as

$$\Delta I_{di} = \left[\frac{K_{c fi}}{(1 + S T_{dci})} \right] * \Delta f \quad (25)$$

Where, $i=1,2$.

Where ΔI_{di} is the incremental change in current of CES unit(KA), T_{dci} is the converter time delay(second), $K_{c fi}$ is the gain of the control loop(KA/Hz), S is the Laplace operator(d/dt) and I denotes the area.

4.2 Area Control Error (ACE) as Control Signal

In case of the tie line power deviation signals are available; it may be desirable to use area control error as input to CES control logic. It has certain advantages, compared to frequency deviation as control signal, which are described later. The area control error of two areas are defined as

$$ACE_i = \Delta P_{ij} + B_i * \Delta f_i \quad (26)$$

Where, $i=1,2$, Δf_i = Change in frequency of area, i . ΔP_{ij} = Change in tie line power flow out of area i to j . If ACE is

directly used for the control of CES, The gains constant K_{ci} (KA/unit Area) would be totally different from K_{cf} , the gain constants for frequency as control signal. So a signal proportional to area control error $(\Delta f_i + (1/B_i) * \Delta P_{ij})$ is used in such a scheme. Then,

$$\Delta I_{di} = \frac{K_{cai}}{(1 + ST_{dci})} (\Delta f_i + \frac{1}{B_i} * \Delta P_{ij}) \quad (27)$$

where $i, j=1, 2$.

The capacitor voltage deviation can be sensed and used as a negative feed back signal in the CES control loop to achieve quick restoration of voltage then, that with frequency deviation as control signal,

$$\Delta I_{di} = \frac{1}{(1 + ST_{dci})} (K_{cfi} \Delta f_i - k_{vdi} \Delta E_{di}) \quad (28)$$

Where K_{vdi} (KA/KV) is the gain corresponding to the ΔE_d feedback. The block diagram representation of such a control scheme is shown in Fig. 3.

5. Neural Network

Back-propagation Algorithm: The sequential updating of weights is the preferred method for on-line implementation of the back-propagation algorithm. For this mode of operation, the algorithm cycles through the training sample $\{X(n), d(n)\}_{n=1}^N$ as follows:

- (i) Initialization: Assuming that no prior information is available, pick the synaptic weights and thresholds from a uniform distribution whose mean is zero and whose variance is chosen to make the standard deviation of the induced local fields of the neurons lie at the transition between the linear and saturated parts of the sigmoid activation function.
- (ii) Presentations of Training Examples: Present the network with an epoch of training examples. For each example in the set, ordered in some fashion, perform the sequence of forward and backward computations described under points (iii) and (iv), respectively.
- (iii) Forward Computation: Let a training example in the epoch be denoted by $(x(n), d(n))$, with the input vector $x(n)$ applied to the input layer of sensory nodes and the desired response vector $d(n)$ presented to the output layer of computation nodes. Compute the induced local fields and function signals of the network by proceeding forward through the network, layer by layer. The induced local field V_j^l for neuron j in layer l is

$$V_j^l(n) = \sum_{i=0}^{m_0} w_{ji}^l(n) y_i^{l-1}(n) \quad (29)$$

Where: $y_i^{l-1}(n)$ is the output signal of neuron i in the previous layer $l-1$ at iteration n .

$w_{ji}^l(n)$ is the synaptic weight of neuron j in layer l that is fed from neuron i in layer $l-1$

$w_{ji}^l(n) = b_j^l(n)$ is the bias applied to neuron j in layer l

Assuming the use of sigmoid function, the output signal of neuron j in layer l is

$$y_j^l = \Phi_j(v_j(n)) \quad (30)$$

if neuron j is in the first hidden layer (i.e. $l=1$), set

$$y_j^0 = x_j(n) \quad (31)$$

Where $X_j(n)$ is the j^{th} element of the input vector $x(n)$. If neuron j is in the output layer, set

$$y_j^l = o_j(n) \quad (32)$$

Compute the error signal

$$e_j(n) = d_j(n) - o_j(n) \quad (33)$$

Where $d_j(n)$ is the j^{th} element of the desired response vector.

(iv) Backward Computation: Compute the δ s (local gradients) of the network, defined by

$$\delta_j^l(n) = e_j^l(n) \Phi_j'(v_j^l(n)) \quad (34)$$

$$\delta_j^l(n) = \Phi_j'(v_j^l(n)) \sum_k \delta_k^{l+1}(n) w_{kj}^{(l+1)}(n) \quad (35)$$

Where the prime in $\Phi_j(\cdot)$ denotes differentiation with respect to the argument. Adjust the synaptic weights of the Network in layer l according to the generalized delta rule:

$$w_{ji}^l(n+1) = w_{ji}^l(n) + \alpha [w_{ji}^l(n-1)] + \eta \delta_j^l(n) y_i^{l-1}(n) \quad (36)$$

Where η is the learning rate parameter and α is the momentum constant.

Iteration: Iterate the forward and backward computations under points (iii) and (iv) by presenting new epoch of training examples to the network until the stopping criterion is met. The order of training examples should be randomized from epoch to epoch. The momentum and learning-rate parameter are typically adjusted (and usually decreased) as the number of training iterations increase. There are three states for the single area AGC. Δf - change in frequency of the plant output, ΔP_T - change in turbine power, ΔP_H - change in hydraulic amplifier power.

Neural Network Controller:

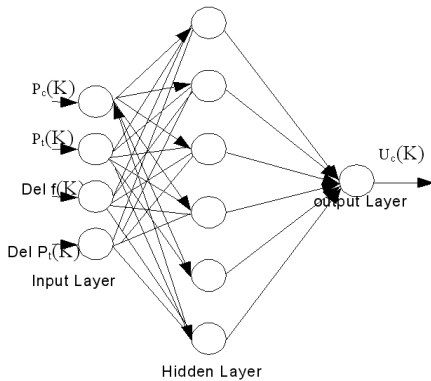


Fig. 3. Architecture of ANN controller for single area AGC.

Hence, $X_p = [\Delta f \quad \Delta P_T \quad \Delta P_H]$
 At steady state, $\Delta f = 0.0$, $\Delta P_T = \Delta P_E$, and $\Delta P_H = \Delta P_E / K_{T1}$

The internal architecture of the neural network controller is shown in the above Fig. 3. The neural network consists of one input layer, one hidden layer of 20 neurons, and one output layer. In case of controller for single area system, we have one neuron at the output layer. In case of two area system, we use two neurons in the output layer for getting separate control inputs to the individual areas. In the input layer, we have got four nodes (in case of single area system). Three nodes are for the state inputs:-change in frequency (Δf), change in hydraulic power (ΔP_h), change in turbine power (ΔP_t) and fourth node for receiving the load estimate as input. Note that all the values are in per unit (P.U). The output neuron generates the control input to the plant (U_c). The activation functions used are hyperbolic tangent functions for each neuron. Figure 3 is essentially composed of a layered arrangement of controller and plant equations blocks. The controller is a neural network. If the block containing the plant equations, P, were replaced by a neural network copy, the unraveled system of Fig. 3 would become a giant layered neural network with inputs $X_p(0)$ and ΔP_E , output $X_p(K)$, and desired output $X_d(K)$. The back propagation algorithm could then be applied to train such a network. By doing so, the error gradient defined at the output of the network are back-propagated through the the neural network copy of the plant and C blocks, from $X_p(K)$ back to $X_p(0)$; hence, the name back propagation through-time. This approach was first introduced by Nguyen and Windrow (1989), and was successfully applied to number of applications in the area of nonlinear neural control. In this paper, we adopt a slightly different approach by which we avoid the introduction and training of a neural network copy of the plant equations. The basic idea is that instead of building a neural network copy or emulator of P to back - propagate error gradients through it, it is possible to directly back propagate the error gradients through the plant equations P. Building a neural network emulator of the plant and back propagating error gradients through it is nothing other than

approximating the true Jacobian matrix of the plant using a neural network technique. Whenever the equations of the plant are known beforehand, they can be used to compute, analytically or numerically, the elements of the Jacobian matrix. The error gradient at the input of the plant is then obtained by multiplying the output error gradient by the Jacobian matrix.

The inputs for ANN in two area AGC are the states of the plant.

$$X_p = [\Delta f_i, \Delta P_{T1}, \Delta P_{H1}, \Delta f_2, \Delta P_{T2}, \Delta P_{H2}, \Delta P_{12}]$$

$$\Delta P_{E1}' = \Delta P_{E1} \quad \Delta P_{E2}' = \Delta P_{E2}$$

Where, ΔP_{E1} is the load perturbation in area 1, ΔP_{E2} is the load perturbation in area 2. For Training the vector X_p was initially set to,

$$X_p = [0.0 \quad 0.0 \quad 0.0 \quad 0.0 \quad 0.0 \quad 0.0 \quad 0.0]$$

The Target Output states of the plant during steady state are $X_d = [\Delta f_1=0, \Delta P_{T1}=(\Delta P_{E1}+\Delta P_{12}), \Delta P_{H1}=(\Delta P_{E1}+\Delta P_{12})/K_{T1}, \Delta f_2=0, \Delta P_{T2}=(\Delta P_{E2}-\Delta P_{12}), \Delta P_{H2}=(\Delta P_{E1}-\Delta P_{12})/K_{T2}, \Delta P_{12}=0]$

6. Stability of Control Loops

The calculation of linearized system eigen values is done separately for the case where the SMES, or the CES control is active. The calculated eigen values are presented in Table 1, 2 & 3. Table 1 compares the calculated eigen values of two area power system with and without controller. The calculated eigen value shows that for open loop, the system unstable because eigen values lies in right half of S plane and for the case of integral controller the system is stable. Table 2 shows that when the SMES loop is present system is stable and it reduces settling time, peak over shoot, similarly Table 3 compares the calculated eigen values of power system with different cases, open loop, with SMES, with CES. The eigen values of Table 3 demonstrates the satisfactory behaviors of power system. For stability analysis eigen values for two area open loop eigen values, with integral controller without SMES, with SMES, CES have been calculated separately. From this analysis AGC for two area with CES is better than AGC with SMES has been calculated. After this proposed controller CES and SMES has been compared properly.

Table 1. Eigen Values

S.N	Open Loop	PI controller
1.	-72.5	-73.8646
2.	-19.99	-19.995
3.	8.0031	-3.9985
4.	0.0026	-0.0062
5.	0.2405	-1.6406
6.	0.4568	-0.5095 + 0.6308i
7.	0.7958	-0.5095-0.6308i

Table 2. Eigen values using SMES

S.N	Open Loop	PI controller	With SMES
1.	-72.5	-73.8646	-76.8646
2.	-19.99	-19.995	-33.2545
3.	8.0031	-3.9985	-19.9985
4.	0.0026	-0.0062	-5.0062
5.	0.2405	-1.6406	-1.6406
6.	0.4568	-0.59 + 0.638i	-0.5095 + 0.638i
7.	0.7958	-0.59-0.638i	-0.5095 - 0.638i
8.	-	-	-0.0000
9.	-	-	-0.0755

Table 3. Eigen Values Using SEMS & CES

S.N	Open Loop	With SMES	With CES
1.	-72.5	-76.8646	-82.8646
2.	-19.99	-33.2545	-37.2545
3.	8.0031	-19.9985	-33.9985
4.	0.0026	-5.0062	-25.0062
5.	0.2405	-1.6406	-21.6406
6.	0.4568	-0.509 + 0.638i	-5.5095 + 8.638i
7.	0.7958	-0.509 - 0.638i	-5.5095 - 8.638i
8.	-	-0.0000	-0.2000
9.	-	-0.0755	-2.0705

7. Result Analysis

In this study, an application of ANN controller for load frequency control in power system is investigated. For the purpose, the interconnected power system having two areas consist of steam turbines is considered. First the load frequency control in power system is simulated by using both ANN and conventional controller to compare the behaviors of the controllers. In this simulation, a step load increasing in the first area of power system is considered, only one ANN controller, which controls the input of each area in power system together, is considered. Back propagation through time algorithm is used as neural network learning rule to cope with the continuous time dynamics. In Table 4, 5 shows frequency deviation in single, two area of power system against to the load disturbance mentioned above are shown for using ANN controller and conventional integral

Table 4. Comparison table for integral and ANN controller for Single Area power system

Load in %	Integral controller		ANN controller	
	Time (sec)	Δf (Hz)	Time (sec)	Δf (Hz)
1	8.7	-0.000182	2.4	-0.000182
10	10.83	-0.000512	3.5	-0.000512
-1	12.78	0.000016	2.8	-0.000091
-10	11.18	0.000424	2.5	-0.000468
50	9.37	-0.006025	1.7	-0.005073
-50	9.37	0.006025	4.1	0.009031

Table 5. Comparison table for Integral and ANN controller responses for Two Area power system

Load in %	Integral controller Response				ANN controller Response			
	Area 1		Area 2		Area 1		Area 2	
	T (s)	Δf (Hz)	T (s)	Δf (Hz)	T (s)	Δf (Hz)	T (s)	Δf (Hz)
10	36	0.03	36	0.03	31	0.003	31	0.0003
-1	43	0.06	43	0.06	43	0.009	43	0.0009
-10	42	0.02	42	0.02	42	0.002	42	0.0002
50	45	0.03	45	0.03	45	0.003	45	0.0003
-50	20	0.02	20	0.02	20	0.002	20	0.0002

controller, respectively. From this Table 4, 5, it is seen that the ANN controller is superior than conventional controller against to the step load disturbance increasing in the single and two areas.

Further to damp out these oscillations AGC is implemented with SMES units in each area. These simulation results are carried out while SMES is present in each area of the power system, according to deviation of the power system energy demand, the SMES unit releases the needed energy or absorbs residue energy form power system. The model including generation unit and SMES unit together represents realistic performance of power system. So non linear state equation of the power system are used directly during the control of power system by ANN and integral controller. From the obtained results Table 6 & 7 shows that the performance of ANN controllers is better than conventional controller and also the positive effect of SMES unit on AGC is presented and SMES reduces settling and peak overshoot.

Table 6. Comparative table for ANN based single areas AGC with/without SMES for various disturbances

Load in %	Without SMES		With SMES	
	Time (sec)	Δf in Hz	Time (sec)	Δf (Hz)
1	2.4	-0.000182	1.5	-0.000151
10	3.5	-0.000512	2.0	-0.000452
-1	2.8	-0.000091	1.8	-0.000085
-10	2.5	-0.000468	1.9	-0.000365
50	1.7	-0.005073	1.5	-0.003562
-50	4.1	0.009031	3.0	0.00731

Table 7. Comparative table for ANN based two areas AGC with/without SMES for various disturbances (1%, 10%, 50%, -1%, -10%, -50%)

Without SMES				Including SMES			
Area 1		Area 2		Area 1		Area 2	
T (s)	Δf (Hz)	T (s)	Δf (Hz)	T (s)	Δf (Hz)	T (s)	Δf (Hz)
38	0.001	38	0.0001	1.5	-0.0001	1.5	0.0001
36	0.003	31	0.0003	1.6	-0.0006	1.5	0.0005
43	0.006	43	0.0009	1.5	-0.003	1.5	0.0029
42	0.002	42	.00002	1.5	0.0001	1.5	0.0001
45	0.003	45	.00003	1.5	0.0006	1.5	0.0005
20	0.002	20	.00002	1.0	-0.0001	1.0	0.0001
20	0.028	20	.00028	1.0	-0.001	1.0	-0.001

The validity of superconducting magnetic energy storage and battery energy storage for power system dynamics performance improvement has been widely reported in [10]-[18]. Their applications in real power system have invited problems from the view point of operation, maintenance and cost involvement but capacitive energy storage (CES) is a better choice to damp out power system oscillations, following any perturbation in power system. CES is practically, maintenance free, unlike other energy storage devices, and CES does not impose any environment problem. The operation is quite simple and less expensive. Thus a corrective measure against power system perturbation, CES plays an important role to damp out local modes of oscillations.

Table 8 shows performance evaluation of CES with two areas is considered. From this table it is noted that due to the application of CES action for either 10% to 50% step disturbance. Under this condition, the stored energy in CES is almost immediately released through the power conversion system to the grid. Thus, application of capacitive energy stored unit quickness the transient stability phenomena even after the occurrence of a fault and subsequent clearance of the same and it may be successfully practically implemented for improving small signal dynamic performance of power system.

Table 8. Time Vs Δf for two areas AGC with SMES & CES for Various disturbances 1%, 10%, 50%, 75%, -1%, -10%,-50%, -75%)

With SMES				With CES			
Area 1		Area 2		Area 1		Area 2	
T (s)	Δf (Hz)	T (s)	Δf (Hz)	T (s)	Δf (Hz)	T (s)	Δf (Hz)
1.5	-0.0001	1.5	0.0001	1.4	0.0005	1.4	.0005
1.6	-0.0006	1.5	0.0005	1.5	0.0004	1.5	0.0004
1.5	-0.003	1.5	0.0029	1.3	0.0003	1.3	0.0003
1.5	0.0001	1.5	0.0001	1.2	0.0003	1.2	0.0003
1.5	0.0006	1.5	0.0005	1.2	0.0004	1.2	0.0004
1.0	-0.0001	1.0	-0.0001	0.8	0.0003	0.8	0.0003
1.0	-0.001	1.0	-0.001	0.8	0.0005	0.8	0.0005

8. Conclusions

This study is an application of ANN to automatic generation control, in a power system, having SMES and CES. In this work, transient behaviors of the frequency of each area and tie line power deviation in the power system with two areas, are considered, under any load disturbances in any area. In practice, power system generally has more than two areas, and each area is different from others. But, in this study, the power system, of two thermal areas, is considered. The nonlinear state space equation of power system is obtained and these equations are used directly during the control of power system by both integral controller and ANN controllers. This is not an usual method with ANN controller. When ANN used in order to back propagate the error, ANN emulator is used, instead of

power system, in most cases. ANN with back propagation through time algorithm is used as controller and power system is modeled by its state space equations. In this work the obtained simulation results show that the performance of ANN with CES is better than conventional controller, with energy storing devices and ANN with SMES controller.

References

- [1] J. K. Cavin, M.C. Budge, and P.Rosmusen, "An optimal linear system approach to load frequency control", *IEEE Trans. On power apparatus and system*, Vol.90, pp. 2472-2482, 1971.
- [2] N.N.Benjamin and W.C.Chang, "Multilevel load frequency control of interconnected power system", *Proc, IEE*, Vol. 125, pp. 521-526, 1978.
- [3] J.Nanda abd B.L.Kavi, "Automatic Generation control of interconnected power system," *Proc, IEE*, Vol. 125, No.5, pp.385-390, 1988.
- [4] D.Das, J.Nanda, M.L.Kothari, and D.P.Kothari, "Automatic generationcontrol of hydro thermal system with new control error considering generation rate constraint," *Electric machines and power system*, Vol.18, pp. 461-471, 1990.
- [5] N.N.Benjamin and W.C.Chang, "Variable structure control of electric power generation," *IEEE Trana.on power Apparatus and System*, Vol. 101, No.2, pp. 376-380, 1982.
- [6] S. Haykin, "Neural Networks: A Comprehensive Foundation" 2nd edition, 2006.
- [7] D.H. Nguyen and B.Widrow, 1990, "Neural Networks for Self learning Control system," *IEEE Control Systems Mag.*, pp.18-23, 1990.
- [8] D. H. Nguyen and B. Widrow, "Neural networks for self-learning control systems," *IEEE Control Systems Mag.*, pp. 18-23, 1990.
- [9] S. C. Tripathy, R. Balasubramania, and N. P. S. Chanramohanan, "Effect of superconducting magnetic energy storage on automatic generation control considering governor deadband and boiler dynamics," *IEEE Trans. on Power System*, Vol. 7, No. 3, pp. 1266-1273, 1992.
- [10] A. Demiroren, N. S. Sengor, and H. L. Zeynelgil, "Automatic generation control by using ANN technique," *Electric Power Components and systems (Electric Machines and Power Sytems)*, Vol. 29, No. 10, pp. 883-896, 2001.
- [11] F.Beaufays, Y. A. Magid, and B. Widrow, 1994," *Application of Neural Network to Load Frequency Control in Power System*," *Neural Networks*, Vol.7, No.1, pp.122-128, 1989.
- [12] A. Demiroren, N.S.Sengor, and H.L.Zeynelgi, "Automatic generationcontrol by using ANN technique," *Electric Power Component and Systems*. Vol.29, No.10.pp.883-896,2001.
- [13] H.L.Zeynelgil, A. Demiroren, and N.S.Senger, "Load Frequency control for power saystem with reheat

steam turbine and governor dead band normality by using Neural Network Controller,” *European Transaction on Electrical power (ETEP)*, Vol.12, No. 3, pp.179-185, 2002.

- [14] O.I.Elgerd, *Electric Energy System Theory: An Introduction*, McGraw – Hill Book Company, 1971.
- [15] H.J.Kunish, K.G.Krammer and H.Domonic “Battery Energy Storage-Another Option for Load Frequency Control & Instantaneous reserve”, *IEEE Trans on Energy conversion* Vol. E-1, No. 3. pp41-46, Sep 1986.
- [16] H.J.Boeniig & J.F.Haur,”Commissioning tests of the Bonneville power Administration 30 MJ super conducting Magnetic storage unit”, *IEEE Trans on power apparatus & systems*. Vol. PAS-104, No. 2. PP.302-312. Feb 1982.
- [17] Banarjee.J.K, Chatterjee and S.C.Tripathy, “Application of Magnetic energy storage units as Load Frequency Control Stabilizers”, *IEEE Trans, on energy conversion*, Vol. 5, No. 1, pp.481-501, March 1990.
- [18] Kwa-Sur Tam and Prem kumar,” Application of super magnetic energy storage in an asynchronous link between power system”, *IEEE Trans on Energy conversion*, Vol. 5, No. 3, Sep 1971.
- [19] H.A. Peterterson, N.Mohan and R.W.Boom, “Super Conductive energy storage Inductor-Converter Units for power system”, *IEE Trans. On Powerapparatus and systems*, Vol. PAS-94, No. 4, PP 1337-1348, July/August 1975.
- [20] R.J. Loyd, J.D.Rogers et al., “A feasibility utility scale superconducting Magnetic Storage Plant”, *IEEE Trans. On Energy conversion*, Vol. EC-1, No. 4, PP. 63-64, December 1986.
- [21] Y.Mitani, K.Tsuji, Y.Murakami, “Application of Superconducting Magnetic Energy storage to improve power system dynamic performance,” *IEEE trans. On power system*, Vol. 3, No. 4-1988.
- [22] S.C. Tripathy, R.Balasubramaniam, P.S. Chandramohan Nair, “Effect of Superconducting Magnetic Energy Storage on Automatic Generation Control Considering Governor Dead band and Boiler dynamics.” *IEEE tran. On power system* Vol 7, Aug 1992.
- [23] S.C. Tripathy, K.P. Juengst, Sampled data automatic generation control with superconducting magnetic energy storage in power systems, *IEEE Trans. Energy Convers.* 12 (June (2)) (1997) 187-192.
- [24] S. Banerjee, J.K. Chatterjee, S.C. Tripathy, Application of magnetic energy storage unit as load frequency stabilizer, *IEEE Trans. Energy Convers.* 5 (March (1)) (1990) 46-51.



J.Raja born on 1980 and received his B.E.degree (Electrical and Electronics) and M.E. degree (Power System) in the year 2001 & 2003 respectively ,He is currently pursuing his Ph.D degree in Pondicherry University, Puducherry, India. He published technical papers in International & National Journals and Conferences. He is currently working as Assistant Professor in the Electrical & Electronics Engineering Department at Sri Manakula Vinayagar Engineering College, Affiliated to Pondicherry University, Pondicherry, India. His area of interest is power system Controls and Stability, operational planning and control. He acquired Member in ISTE in India.



C.Christofer Asir Rajan born on 1970 and received his B.E. (Distn.) degree (Electrical and Electronics) and M.E. (Distn.) degree (Power System) from the Madurai Kamaraj University (1991 & 1996), Madurai, India. And he received his postgraduate degree in D.I.S. (Distn.) from the Annamalai

University, Chidambaram. He received his Ph.D degree in Power System from the College of Engineering, Guindy, Anna University, Chennai, India (2001-2004). He published technical papers in International & National Journals and Conferences. He is currently working as Associate Professor in the Electrical & Electronics Engineering Department at Pondicherry Engineering College, Pondicherry, India. His area of interest is power system optimization, operational planning and control. He is undertaking various R & D projects. He acquired Member in ISTE and MIE in India.

Appendix-1

System Data:

$P_{r1}=P_{r2}=1200\text{MW}$, $T_{p1}=T_{p2}=20\text{s}$, $K_{p1}=K_{p2}=120\text{Hz/p.u.MW}$,
 $T_{r1}=T_{r2}=10\text{s}$, $K_{r1}=K_{r2}=0.5$, $T_{i1}=T_{i2}=0.3\text{s}$, $T_{12}=0.0866\text{s}$,
 $T_{g1}=T_{g2}=0.08\text{s}$, $R_1=R_2=2.4\text{Hz/pu.MW}$, $D_1=D_2=8.33*10^{-3}$
 puMW /Hz , $P1=0.01\text{pu/MW}$, $P2=0.0\text{pu/MW}$.

Super Conduction Magnetic Energy Storage Data:

$K_f=100\text{KV/unit MW}$, $K_{id}=0.20\text{KV/KA}$, $K_{Ai}=0.875$, $L=2.65\text{H}$,
 $T_{dc}=0.03\text{s}$, $I_{ido}=4.5\text{KA}$.

Capacitive Energy Storage Data:

$C=1\text{farad}$, $R=100\text{ohm}$, $T_{dc}=0.05\text{s}$, $K_{acc}=70\text{KA/unit MW}$,
 $K_{vd}=0.1\text{KA/KV}$, $V_{do}=2\text{KV}$.